Thermo-électricité

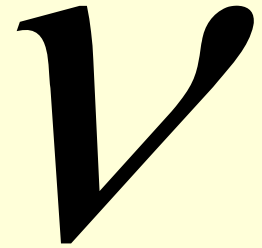## Effet Seebeck - Effet Peltier

Introduction et effets quantiques
à l'échelle mésoscopique.

Jean-Louis Pichard

IRAMIS / SPEC

CEA-Saclay

Rendement

ν

$$\nu = \frac{W}{Q} = \nu_{Carnot}\left[\frac{\sqrt{ZT+1}-1}{\sqrt{ZT+1}+\dfrac{T_C}{T_H}}\right]$$

W :   Puissance obtenue

Q :   Chaleur extraite de la source chaude

T_C, $T_{H:}$ Températures des sources froide et chaude

$$\nu_{Carnot} = 1 - \frac{T_C}{T_H}$$ Rendement de Carnot

ZT   Facteur de mérite

$$ZT = S^2 \frac{\sigma}{\kappa} T$$

σ Conductivité électrique

κ Conductivité thermique

S : Coefficient Seebeck

T: Temperature

$$ZT \geq 3$$

Réfrigerateurs à effet Peltier compétitifs comparés à ceux avec compresseur

$$\frac{\kappa}{\sigma T} = \frac{\pi^2 k_B^2}{3e^2}$$

Nombre de Lorenz
Gaz d'électrons libres

Régime de réponse linéaire

Q : Courant de chaleur
I : Courant électrique

R : Résistance électrique
K : Conductance thermique

$$- \Delta V = RI + S\Delta T$$

$$Q = \Pi I - K\Delta T$$

Relation de Kelvin-Onsager

Π Coefficient Peltier

$$\Pi = ST$$

S   Coefficient Seebeck (Thermopower)

Conductance et Coefficient Seebeck en fonction de la transmission des électrons au niveau de Fermi

$$G = \frac{1}{R} = \frac{2e^2}{h}\tau(E_F)$$ Landauer - Buttiker

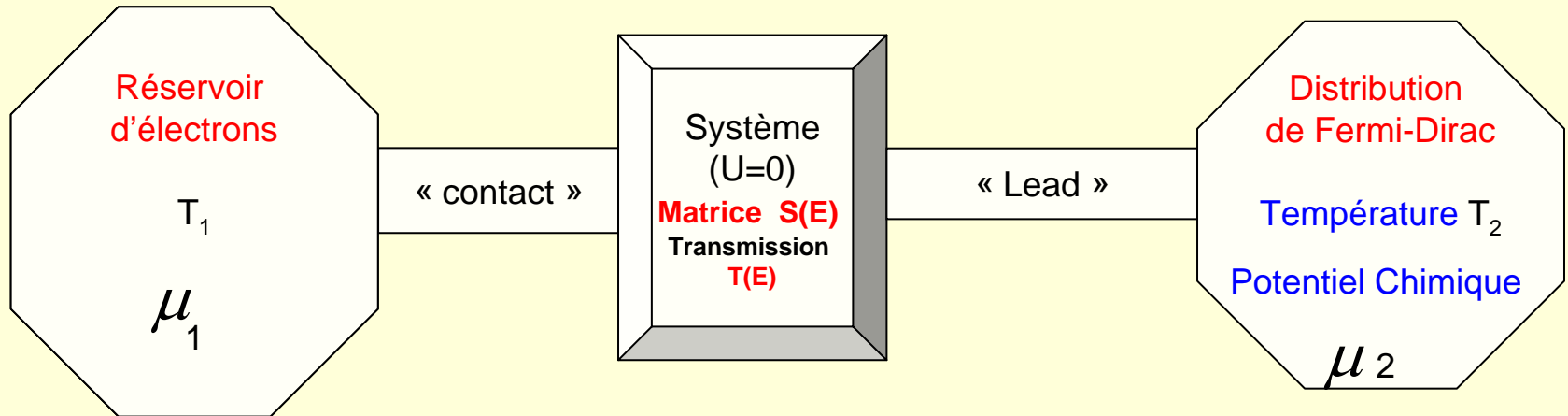$$S = -\frac{\pi^2 k_B^2 T}{3e}\frac{\partial \ln(\tau(E))}{\partial E}\bigg|_{E=E_F}$$ Mott

$$\tau(E) \xrightarrow[N \succ 1]{} tr(tt^+)_{E=E_F}$$ Multi-canaux

Limite $Temperature \longrightarrow 0$

Approche à la Landauer

(Inclure les intéractions U entre électrons dans cette approche est une question délicate)

Réponse linéaire
Courant engendré par un gradient de potentiel électrique
Courant engendré par un gradient de température

S Matrice 2N x 2N

T (= t.t$^+$) Matrice N x N

N nombre de modes dans les « leads »

Courant électrique engendré par un gradient de potentiel électrique entre les 2 réservoirs

$$I = e \int dE.(v(E).\frac{dn}{dE}).T(E).[f(E,\mu_1,T)(1 - f(E,\mu_2,T) - f(E,\mu_2,T)(1 - f(E,\mu_1,T)]$$

$$v(E).\frac{dn}{dE} = \frac{2}{h}$$

$$\Delta\mu = e\Delta V$$

$$\mu_1 = \mu_F$$

$$\mu_2 = \mu_F + e\Delta V$$

$$\frac{I}{\Delta V} = G = (\frac{2e^2}{h}).[\int dE.(-\frac{\partial f}{\partial E})_{\mu_F}.T(E)]$$

$$g_{T\to 0} = \frac{G}{2e^2/h} = T(E_F)$$

$$T(E_F) = \sum_{\alpha\beta}(t.t^+)_{\alpha\beta}\Big|_{E=E_F} = trace\big(t.t^+\big)_{E=E_F}$$

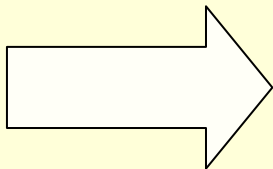# Courant électrique engendré par un gradient de température entre les 2 réservoirs

$$I = \int dE.e.(v(E).\frac{dn}{dE}).T(E).[f(\mu_F,T_1)(1-f(\mu_F,T_2))-f(\mu_F,T_2)(1-f(\mu_F,T_1))$$

$$v(E).\frac{dn}{dE} = \frac{2}{h}$$

$$I = \frac{2e}{h}\int dE.T(E).[f(E,\mu_F,T_1)-f(E,\mu_F,T_2)]$$

Développement de Sommerfeld

(NB: Résonance Kondo)

$$\int dE.T(E).f(E,\mu_F,T) = \int dE.K(E).(-\frac{\partial f(E,\mu_{F,}T)}{\partial E})$$

$$K(E) = \int_{-\infty}^{E} dE'T(E')$$

$$K(E) = K(\mu_F) + \sum_{n=1}^{\infty}[\frac{(E-\mu_F)^n}{n!}][\frac{d^n K(E)}{dE^n}]_{E=\mu_F} \ ?$$

$$\int dE.T(E).f(E) = \int_{-\infty}^{\mu_F} dE.T(E) + \frac{\pi^2}{6}.(k_B T)^2.\frac{dT(E)}{dE}\bigg|_{E=\mu_F}$$

On retrouve la loi de Mott

$$I = \frac{2e}{h} \frac{\pi^2}{6} k_B^2 . (T_1^2 - T_2^2) \frac{dT(E)}{dE} \bigg|_{E=\mu_F}$$

$$\Delta T = T_1 - T_2$$
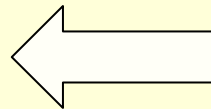
$$T = \frac{T_2 + T_1}{2}$$

$$\frac{I}{\Delta T} = \frac{2e\pi^2 k_B^2}{3h} . T . \frac{dT(E)}{dE} \bigg|_{E=\mu_F}$$

Courant engendré par un gradient de potentiel et de température:

$$I = \frac{2e\pi^2 k_B^2}{3h} . T . \frac{dT(E)}{dE} \bigg|_{E=\mu_F} . \Delta T + \frac{2e^2}{h} . [\int dE . (-\frac{\partial f(E)}{\partial E}) T(E)_{E=\mu}] . \Delta V$$
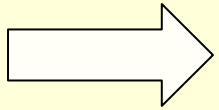
$$I = 0$$

$$S = \frac{\Delta T}{\Delta V} \bigg|_{(I=0)} = -\frac{\pi^2 k_B^2}{3e} T \frac{d \log T(E)}{dE} \bigg|_{E=\mu_F}$$

Loi de Mott

$$T(E_F) \approx \int dE . (-\frac{\partial f(E)}{\partial E}) T(E)_{E=\mu_F}$$

Intérêt d'avoir une haute sensibilité de la conductance
à un changement de la densité électronique

$$ZT \propto T^2 \left(\frac{\partial \tau(E)}{\partial E} \right)^2 \frac{1}{\tau(E)}_{E=E_F}$$

1. Voisinage d'un bord de mobilité (transition métal-isolant)

2 Contacts Quantiques Ponctuels

3 Jonctions moléculaires avec l'énergie de Fermi des électrodes
   près des orbitales moléculaires HOMO et LUMO (highest occupied or
   lowest unoccupied molecular orbitals).

4. Voisinage d'une résonance Kondo

5. …

Observation of Anderson Localization in an Electron Gas

MELVIN CUTLER

Department of Physics, Oregon State University, Corvallis, Oregon 97331

AND

N. F. MOTT

Cavendish Laboratory, Cambridge, England
(Received 21 October 1968)

Anderson has shown that there is no diffusion of an electron in certain random lattices, and Mott has pointed out that, for electrons in materials in which there is a potential energy varying in a random way from atom to atom, Anderson's work predicts that there should be a range of energies at the bottom of the conduction band for which an electron can move only by thermally activated hopping from one localized state to another. An energy E_c will separate the energies where this happens from the nonlocalized range of energies where there is no thermal activation. Cerium sulfide, investigated some years ago by Cutler and Leavy, is a particularly suitable material testing whether this is so because, in the neighborhood of the composition Ce_2S_3, $\frac{1}{9}$ of the cerium sites are vacancies distributed at random, and the number of free electrons can be varied with only very small changes in the number of vacancies. It is shown that the experimental results find a natural explanation in terms of this model: Conduction is by hopping when the concentration of electrons is low and the Fermi energy E_F lies below E_c; but when the concentration is higher and $E_F > E_c$, conduction is by the usual band mechanism with a short mean free path. The thermoelectric power is examined in both ranges, and the Hall mobility in the hopping region ($E_F < E_c$) seems in fair agreement with the theory of Holstein and Friedman.

The corresponding metallic formula for S is, writing $E=E_F$ in both formulas,

$$S = -(\pi^2 k^2 T/3e)d \ln\sigma(E)/dE$$
$$= -\tfrac{1}{3}\pi^2(k/e)[kTd \ln(\mu_0 N)/dE - dW/dE]. \quad (9)$$

Thus, S should be a linear function of T whose slope and intercept yield values of $d \ln(\mu_0 E)/dE$ and (dW/dE) for $E=E_F$. This is found to be true. Some typical linear plots of $S(T)$ are shown in Fig. 5, and the resulting parameters are listed in Table I for all samples for which this analysis could be made.

The above results can be tested for self-consistency in the following way: The parameters derived from $S(T)$ can be used to calculate $(d \ln\sigma/dE)_{E_F}$ at any particular temperature. Dividing this by $(dW/dE)_{E_F}$ yields $(d \ln\sigma/dW)_{E_F}$ at that temperature, which can be compared with a curve for $\ln\sigma$ versus W at that temperature, derived from the resistivity data. We have
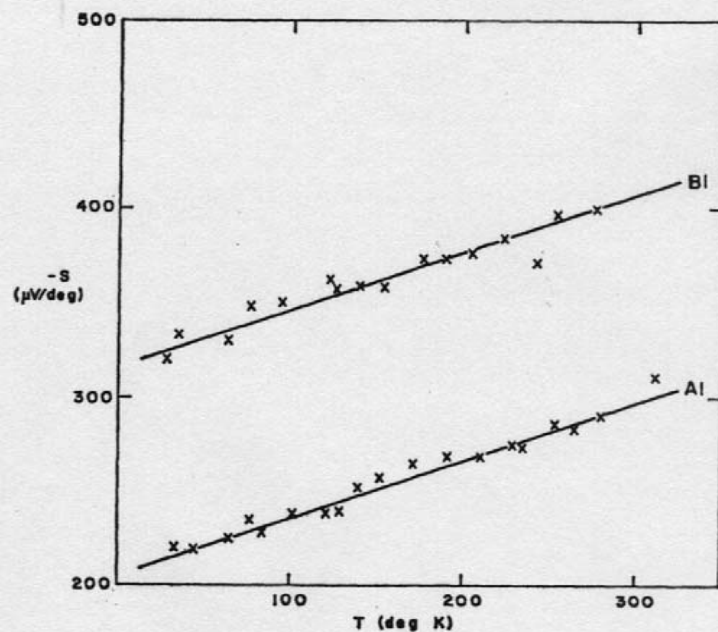

FIG. 5. Some typical plots, showing linear dependence of S on T for samples $A1$ and $B1$.

La conductivité apparait au dessus du bord de mobilité
(mais temperture faible!)

Multichannel Landauer formula for thermoelectric transport with application to thermopower near the mobility edge

U. Sivan and Y. Imry

School of Physics and Astronomy, Tel Aviv University, 69978 Tel Aviv, Israel

Various thermoelectric linear transport coefficients are defined and calculated for two reservoirs connected with ideal multichannel leads and a segment of an arbitrary disordered system. The reservoirs have different temperatures and chemical potentials. All of the inelastic scattering (and, thus, the dissipation) is assumed to occur only in the reservoirs. The definitions of the chemical potentials and temperature differences across the sample itself (mostly due to elastic scattering) are presented. Subtleties of the thermoelectric effects across the sample are discussed. The associated transport coefficients display deviations from the Onsager relations and from the Cutler-Mott formula for the thermopower (although the deviations vanish for a large number of channels and/or high resistance). The expression obtained is used to predict the critical behavior of the electronic thermopower near the mobility edge. It is shown to satisfy a scaling form in the temperature and separation from the mobility edge.

Coefficient Seebeck près d'un bord de mobilité

Cutler-Mott[17] expression, Eq. (40) for the thermopower. However, instead of using the assumptions[15,19] of minimum metallic conductivity for $\sigma(E)$, we invoke the result of the scaling theory[18] that in the vicinity of E_M

$$\sigma(E) = a(E - E_m)^x, \quad E \geq E_m \tag{43}$$

where the exponent x is currently believed to be around unity and a is some constant. Substituting Eq. (43) into Eq. (40) we obtain in the lowest order in temperature $(k_B\theta \ll E_F - E_M)$:

$$s = \frac{k_B}{e} \frac{\pi}{3} \frac{k_B\theta}{E_F - E_m}, \tag{44}$$

while for high temperatures $(k_B\theta \gg E_F - E_m)$ we find

$$\bar{s} = \frac{k_B}{e} \left[\text{const} - \frac{E_F - E_m}{k_B\theta} \right]. \tag{45}$$

Notice however, that the latter limit may be inconsistent with the neglect of inelastic processes. Equations (44) and (45) imply that S can be scaled to depend not on $k_B\theta$ and $E_F - E_M$ separately, but on a single variable $k_B\theta/(E_F - E_M)$.

Coefficient Seebeck
d'un contact quantique ponctuel

Thermometer for the 2D Electron Gas using 1D Thermopower

N. J. Appleyard, J. T. Nicholls, M. Y. Simmons, W. R. Tribe, and M. Pepper

Cavendish Laboratory, Madingley Road, Cambridge CB3 0HE, United Kingdom
(Received 23 July 1998)

We measure the temperature of a 2D electron gas in GaAs from the thermopower of a one-dimensional ballistic constriction, using the Mott relation to confirm the calibration from the electrical conductance. Under hot electron conditions, this technique shows that the power loss by the electrons follows a T^5 dependence in the Gruneisen-Bloch regime, as predicted for acoustic phonon emission with a screened piezoelectric interaction. An independent measurement using conventional thermometry based on Shubnikov–de Haas oscillations gives a T^3 loss rate. We discuss reasons for this discrepancy. [S0031-9007(98)07301-3]
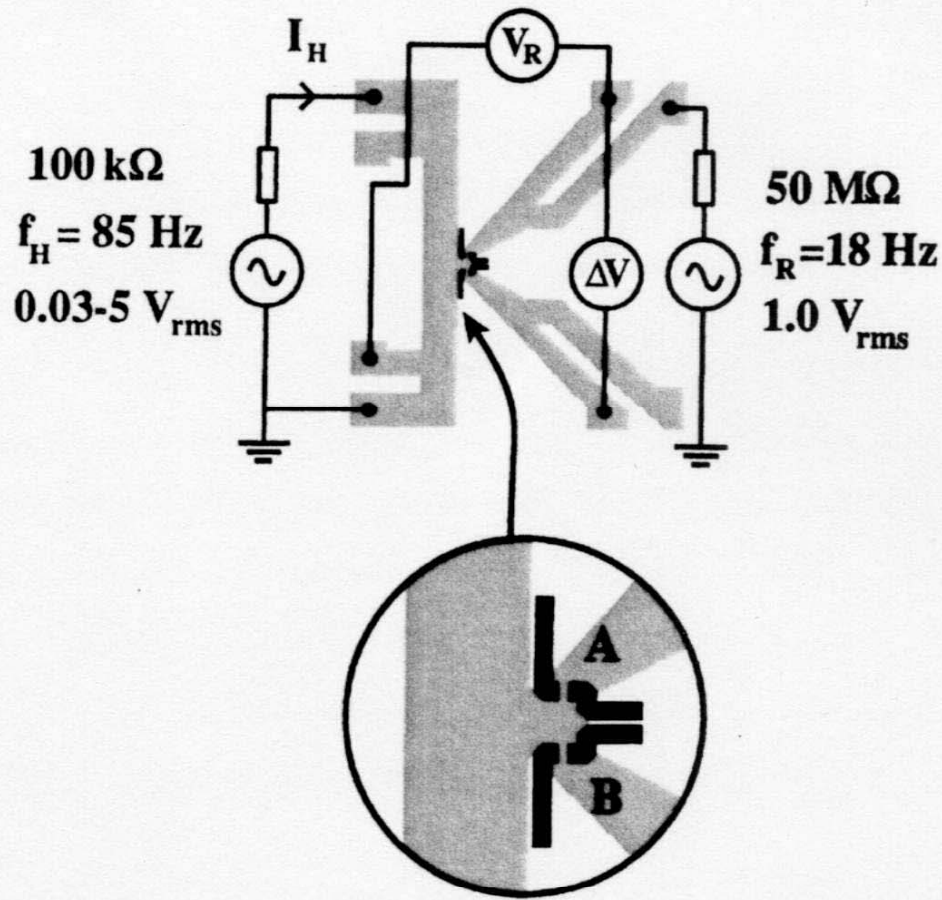
FIG. 1. Schematic of the device and measurement circuit. The etched mesa, shown in grey, consists of a heating channel and two voltage probes, where the two 1D constrictions are defined. The four-terminal resistance R is measured simultaneously with the thermopower S, but at a different frequency. Magnified view: The two pairs of split gates defining the constrictions A and B are shown in solid black.

$L = .4\ \mu m$ and gap width $W = .8\ \mu m$. Because of its thermoelectric properties, the temperature difference $T_e - T_l$ across a 1D constriction generates a potential difference, which is measured [13] at the harmonic frequency $2f_H$. As the 2DEG is heated directly, without raising the lattice temperature T_l, the phonon drag contribution to the thermopower [14] can be ignored and only the contribution of electron diffusion is detected. Figure 1 shows that ΔV is in fact the voltage measured across the two constrictions; one constriction is kept at fixed width as a reference, while the V_g of the other is swept.

When both charge and heat are exclusively carried by electrons, it has been shown both for diffusive [15] and ballistic [16] transport that the thermopower S is related to the energy derivative of the conductance G,

$$S = \left.\frac{\Delta V}{T_e - T_l}\right|_{l=} = -\frac{\pi^2 k_B^2}{3e}(T_e + T_l)\frac{\partial(\ln G)}{\partial \mu}, \quad (1)$$
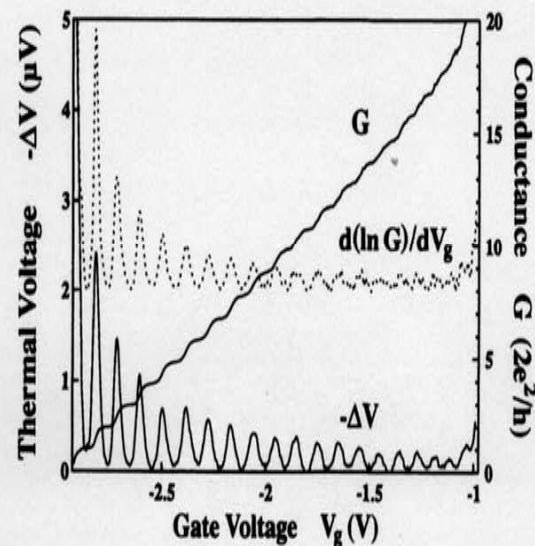

FIG. 2. Experimental traces of the conductance G (derived from R) and the thermopower voltage $-\Delta V$ from constriction A, using a heating current $I_H = 1.5\ \mu A$ at a lattice temperature $T_l = 3\ 5$ mK, so that $T_e \approx 6$ mK. The dashed line shows the predicted thermopower signal $-\Delta V(V_g) \sim d(\ln G)/dV_g$ from the Mott relation [Eq. (1)].

Jonction moléculaire

Thermoelectricity in Molecular Junctions

Pramod Reddy,[1]* Sung-Yeon Jang,[2,3]*† Rachel Segalman,[1,2,3]‡ Arun Majumdar[1,3,4]‡

[1]Applied Science and Technology Program, University of California Berkeley, CA 94720, USA. [2]Department of Chemical Engineering, University of California, Berkeley, CA 94720, USA. [3]Materials Science Division, Lawrence Berkeley Laboratory, Berkeley, CA 94720, USA. [4]Departments of Mechanical Engineering and Materials Science and Engineering, University of California, Berkeley, CA 94720, USA.

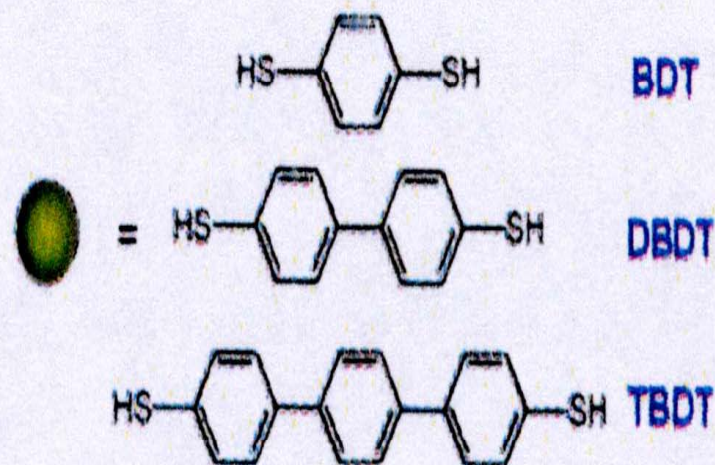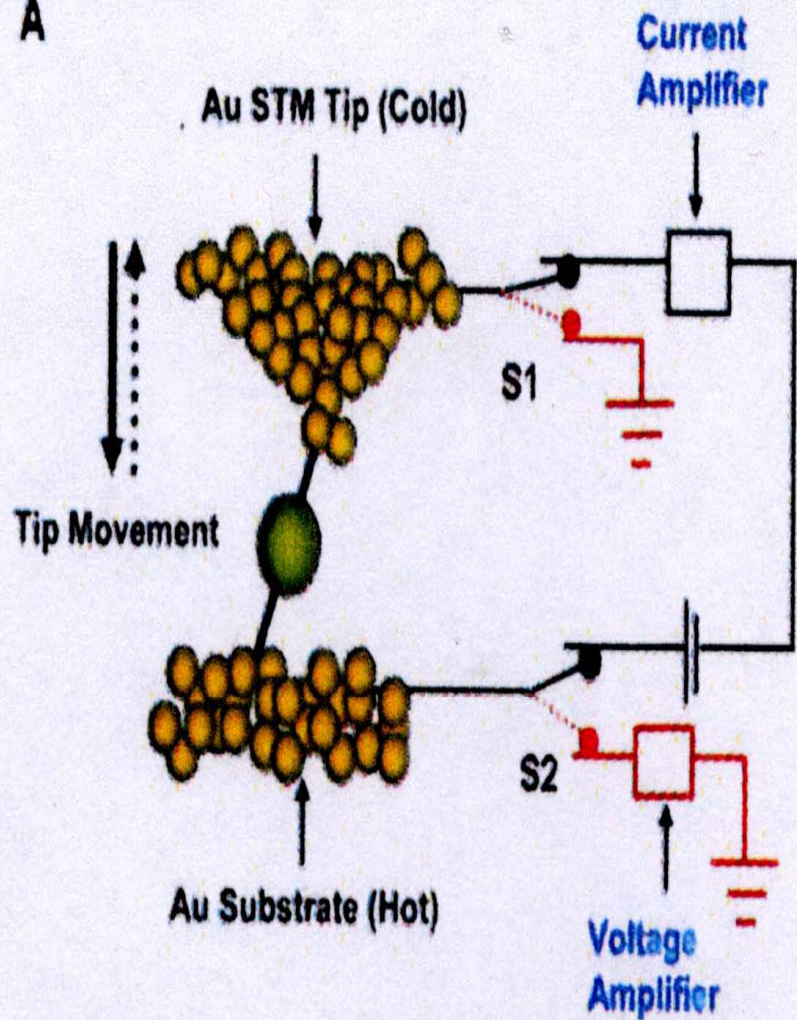*These authors contributed equally to this paper.

†Present address: Optoelectronic Materials Research Center, Korea Institute of Science and Technology, Seoul 136-791, Korea.
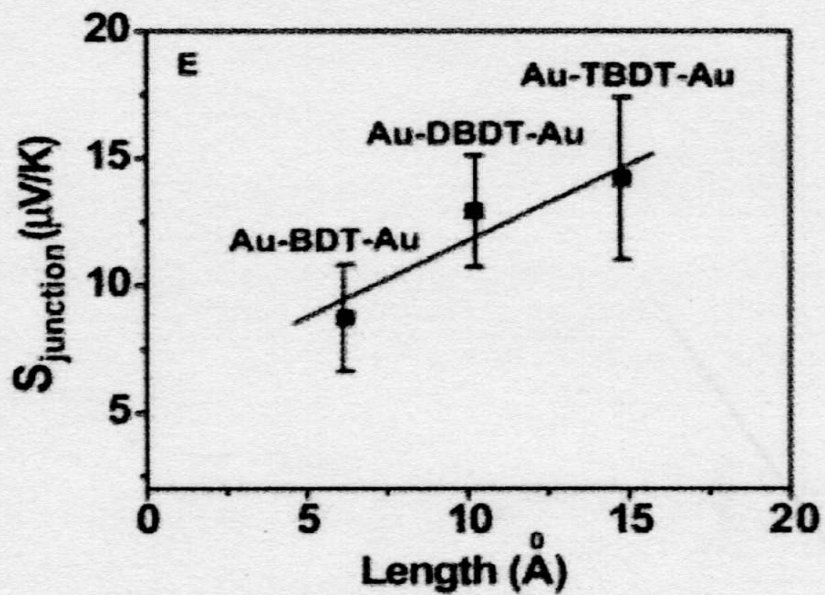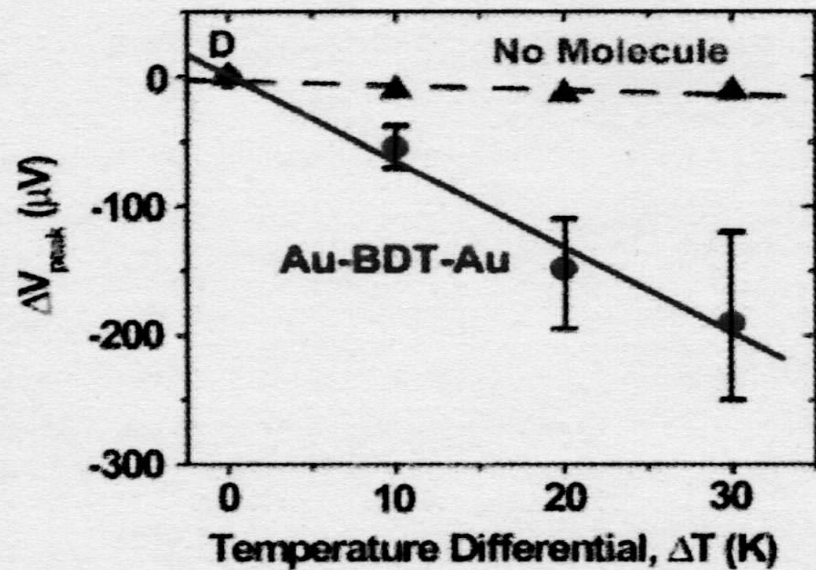
‡To whom correspondence should be addressed. E-mail: majumdar@me.berkeley.edu (A.M.); segalman@berkeley.edu (R.S.)

By trapping molecules between two gold electrodes with a temperature difference across them, the junction Seebeck coefficient of 1,4-benzenedithiol (BDT), 4,4'-dibenzenedithiol (DBDT) and 4,4''-tribenzenedithiol (TBDT) in contact with gold was measured at room temperature to be $(+8.7 \pm 2.1)$ microvolts per Kelvin (μV/K), $(+12.9 \pm 2.2)$ μV/K, and $(+14.2 \pm 3.2)$ μV/K, respectively. The positive sign unambiguously indicates p-type (hole) conduction in these heterojunctions, while the Au Fermi level position for Au-BDT-Au junctions was identified to be 1.2 eV above the highest occupied molecular orbital (HOMO) level of BDT. The ability to study thermoelectricity in molecular junctions provides the opportunity to address these fundamental unanswered questions about their electronic structure while also offering an opportunity to begin exploring molecular thermoelectric energy conversion.

both experimentally (4, 11) and theoretically (7, 12–15), but while some groups suggest that the E_F of the electrodes lies close to the HOMO level (7, 13, 15) other groups contend that E_F lies near the LUMO level (12, 14). Although sweeping the gate bias in single-molecule transistors could potentially yield this information, Coulombic interactions caused by charging of the molecule could perturb the electronic structure (16, 17).

It has been suggested that the sign of the Seebeck coefficient, S, of molecular junctions can indicate the sign of the charge carrier and the relative position of E_F with respect to the HOMO or LUMO levels (8). Indeed, thermopower measurements using a scanning probe microscope have yielded nanoscale spatial distributions of electron and hole concentrations in inorganic semiconductors (18) and have led to chemical potential microscopy at the atomic scale (19, 20). Here we report an alternative approach where we measure S

A

Au STM Tip (Cold)

Current Amplifier

Tip Movement

S1

Au Substrate (Hot)

S2

Voltage Amplifier

HS—⬡—SH BDT

⬤ = HS—⬡—⬡—SH DBDT

HS—⬡—⬡—⬡—SH TBDT

D

No Molecule

Au-BDT-Au

ΔV_{peak} (μV)

Temperature Differential, ΔT (K)

E

Au-TBDT-Au

Au-DBDT-Au

Au-BDT-Au

$S_{junction}$ ($\mu V/K$)

Length (Å)

Micro-Nano Scale Thermal Imaging Using Scanning Probe Microscopy

Li Shi*

Department of Mechanical Engineering
The University of Texas at Austin
Austin, TX 78712
(512) 471-3109 (phone), (512) 471-1045 (fax)
lishi@mail.utexas.edu

Arunava Majumdar

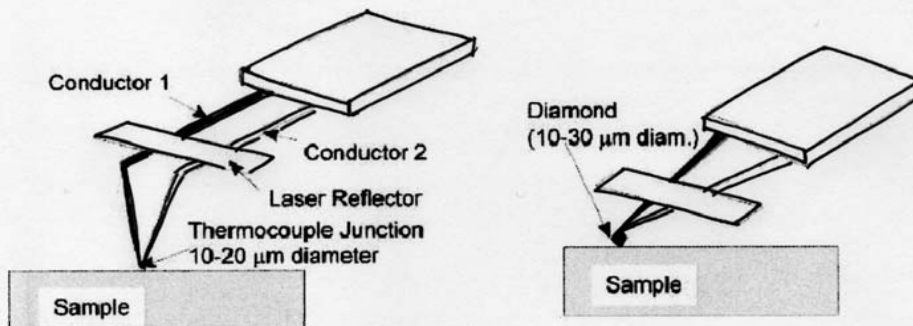Department of Mechanical Engineering
University of California
Berkeley, CA 94706
(510) 643-8199 (phone), (510) 642-6163 (fax)

**Micro-Nano Thermal Imaging using
Scanning Probe Microscopy**

Thermopower of Molecular Junctions: An *ab initio* Study

San-Huang Ke,[1] Weitao Yang,[1] Stefano Curtarolo,[2] and Harold U. Baranger[3]

[1] *Department of Chemistry, Duke University, Durham, NC 27708*
[2] *Department of Mechanical Engineering and Materials Science, Duke University, Durham, NC 27708*
[3] *Department of Physics, Box 90305, Duke University, Durham, NC 27708-0305*

(Dated: August 11, 2008)

Molecular nano-junctions may support efficient thermoelectric conversion through enhanced thermopower.[1,2] Recently, this quantity has been measured for several conjugated molecular nano-junctions with gold electrodes.[3,4] Considering the wide variety of possible metal/molecule systems – almost none of which have been studied – it seems highly desirable to be able to calculate the thermopower of junctions with reasonable accuracy and high efficiency. To address this task, we demonstrate an effective approach based on the single particle green function (SPGF) method combined with density functional theory (DFT) using B3LYP and PBE0 energy functionals. Systematic good agreement between theory and experiment is obtained; indeed, much better agreement is found here than for comparable calculations of the conductance.

The thermoelectric effect – the direct conversion of heat flow produced by a temperature differential to electric voltage or vice versa[5] – might provide an alternative avenue for meeting future energy needs if its efficacy could be improved.[6] The usual figure of merit is $ZT = S^2 T \sigma / \kappa$ where S, T, σ, and κ are the thermopower (Seebeck coefficient), absolute temperature, and electrical and thermal conductivities, respectively. Increasing ZT beyond 1 is a challenging task because the factors S, σ, and κ are interdependent.[6] In recent years, with the advent of nanotechnology, it was found that in nanostructures, such as thin-film and quantum dot superlattices,[7–9] ZT can increase to about 1. The use of molecular junctions is another recent and promising approach.[1–4] In these devices, the electrodes' Fermi energy can be located very close to the highest occupied or lowest unoccupied molecular orbital (HOMO or LUMO, respectively), thus enhancing the thermopower, and
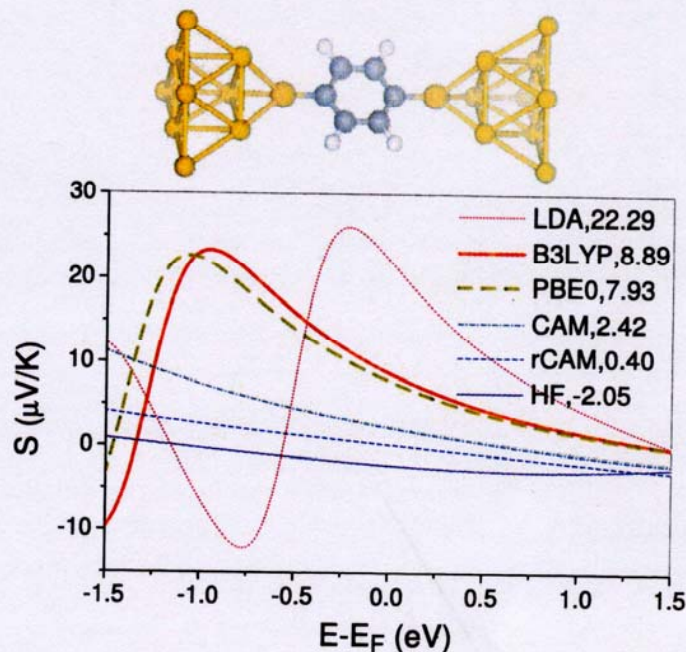

FIG. 1: Thermopower calculated for a benzene-dithiol molecular bridge between two Au leads. Different density functionals are used as specified in the legend. The geometry of the bridge plus 9 Au atoms on either side is optimized; the remaining Au of the semi-infinite leads is included via the wide band limit approximation. Clearly, the calculated thermopower is strongly affected by the density functional used: LDA leads to a Fermi energy close to the HOMO resonance and a large S; in contrast, HF, CAMB3LYP, and rCAMB3LYP place E_F far from the HOMO resonance and so yield a much smaller S. B3LYP and PBE0 give intermediate results which are in good agreement with experimental values at room temperature.
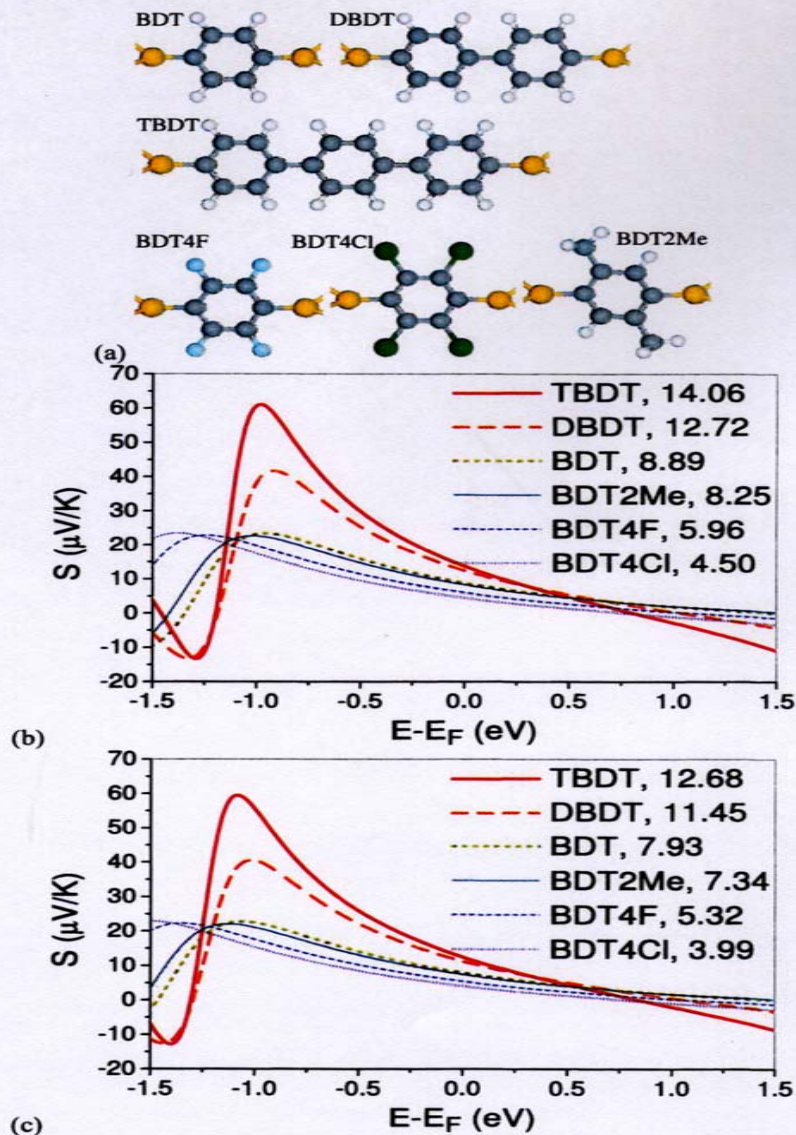
FIG. 2: Thermopower calculated for the molecular junctions shown in (a) using the density functional (b) B3LYP or (c) PBE0. Color code for the atoms: C, H, Au, F, and Cl are black, gray, yellow, blue, and green, respectively. The two functionals yield a remarkably similar form for $S(E)$ and trend among the molecules: TBDT has the largest thermoelectric effect while the two molecules incorporating electron acceptors (F and CL) have the smallest.

Quelques phénoménes mésoscopiques

- Localisation faible
- Fluctuations mésoscopiques (UCF)
- Billiards quantiques
- Blocage de Coulomb
- Effets Kondo (voir Abrikosov)
- Electrons libres et Electrons corrélés
- Phenoménes à N corps quantiques hors équilibre

Aharonov-Bohm-type oscillations of thermopower in a quantum-dot ring geometry

Ya. M. Blanter*
Institut fu¨r Theorie der Kondensierten Materie, Universita¨ t Karlsruhe, 76128 Karlsruhe, Germany
and Theoretical Physics, Moscow Institute for Steel and Alloys, Leninskii pr. 4, 117936 Moscow, Russia
C. Bruder
Institut fu¨r Theoretische Festko¨rperphysik, Universita¨ t Karlsruhe, 76128 Karlsruhe, Germany
Rosario Fazio
Istituto di Fisica, Universita` di Catania, viale A. Doria 6, 95128 Catania, Italy
Herbert Schoeller
Institut fu¨r Theoretische Festko¨rperphysik, Universita¨ t Karlsruhe, 76128 Karlsruhe, Germany
!Received 20 September 1996«

We investigate Aharonov-Bohm-type oscillations of the thermopower of a quantum dot embedded in a ring for the case when the interaction between electrons can be neglected. The thermopower is shown to be strongly flux dependent, and typically the amplitude of oscillations exceeds the background value. It is also shown to be essentially dependent on the phase of the scattering matrix, which is determined by the experimental geometry and is not known in the given experiment. Two procedures to compare theory and experiment are proposed.

Thermoélectricité et EHQ

Observation of Chiral Heat Transport in the Quantum Hall Regime

G. Granger,1 J. P. Eisenstein,1 and J. L. Reno2
1Condensed Matter Physics, California Institute of Technology, Pasadena, California 91125, USA
2Sandia National Laboratories, Albuquerque, New Mexico 87185, USA

Heat transport in the quantum Hall regime is investigated using micron-scale heaters and thermometers positioned along the edge of a millimeter-scale two dimensional electron system (2DES). The heaters rely on localized current injection into the 2DES, while the thermometers are based on the thermoelectric effect. In the ¼ 1 integer quantized Hall state, a thermoelectric signal appears at an edge thermometer only when it is ''downstream,'' in the sense of electronic edge transport, from the heater. When the distance between the heater and the thermometer is increased, the thermoelectric signal is reduced, showing that the electrons cool as they propagate along the edge.

Thermoélectricité et EHQF

Thermopower as a possible probe of non-Abelian quasiparticle statistics in fractional quantum Hall liquids

Kun Yang

Department of Physics and National High Magnetic Field Laboratory, Florida State University, Tallahassee, Florida 32306, USA

Bertrand I. Halperin

Department of Physics, Harvard University, Cambridge, Massachusetts 02138, USA

We show in this paper that thermopower is enhanced in non-Abelian quantum Hall liquids under appropriate conditions. This is because thermopower measures entropy per electron in the clean limit, while the degeneracy and entropy associated with non-Abelian quasiparticles enhance entropy when they are present. Thus thermopower can potentially probe non-Abelian nature of the quasiparticles, and measure their quantum properties.

Scanning Gate Microscopy
of a Nanostructure
inside which electrons interact

Axel Freyn, Ioannis Kleftogiannis

and Jean-Louis Pichard

Scanning gate microscope
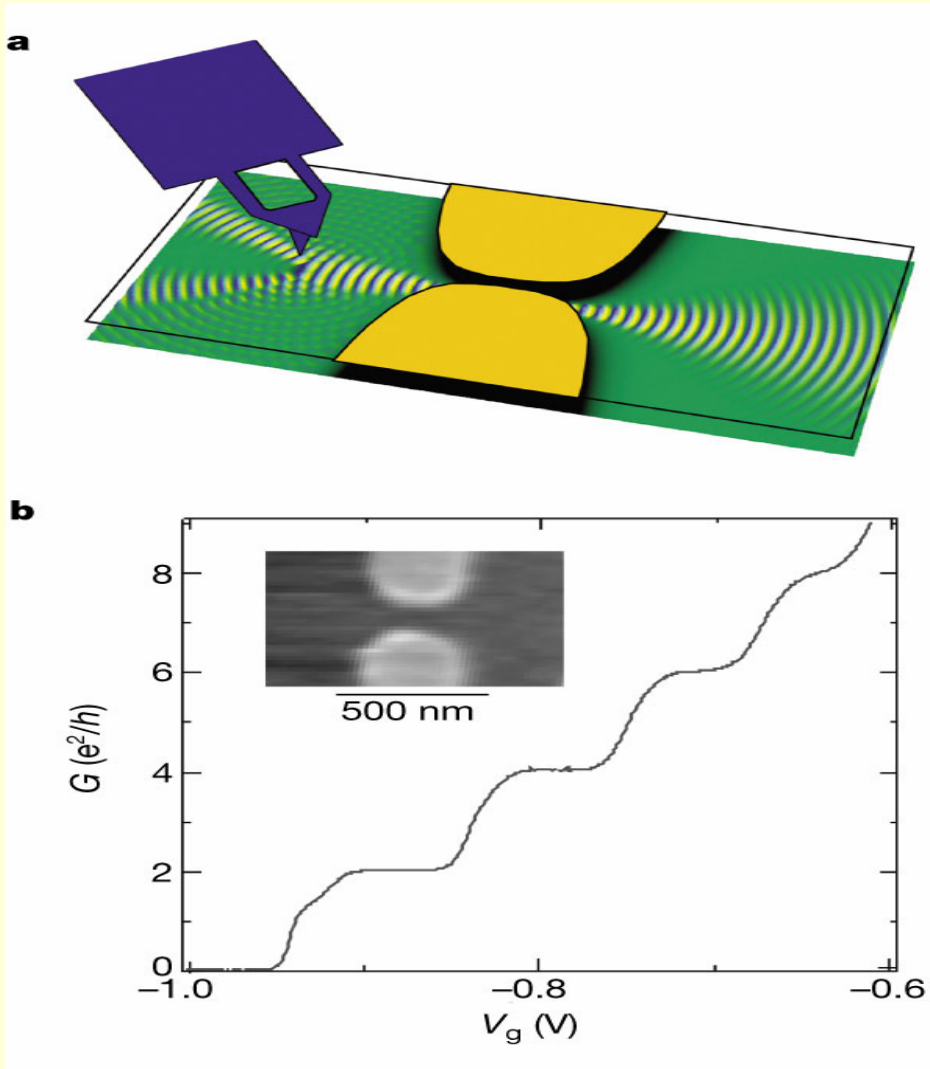
2DEG , **QPC**
AFM cantilever

The charged tip creates a depletion region inside the 2deg which can be scanned around the nanostructure (qpc)
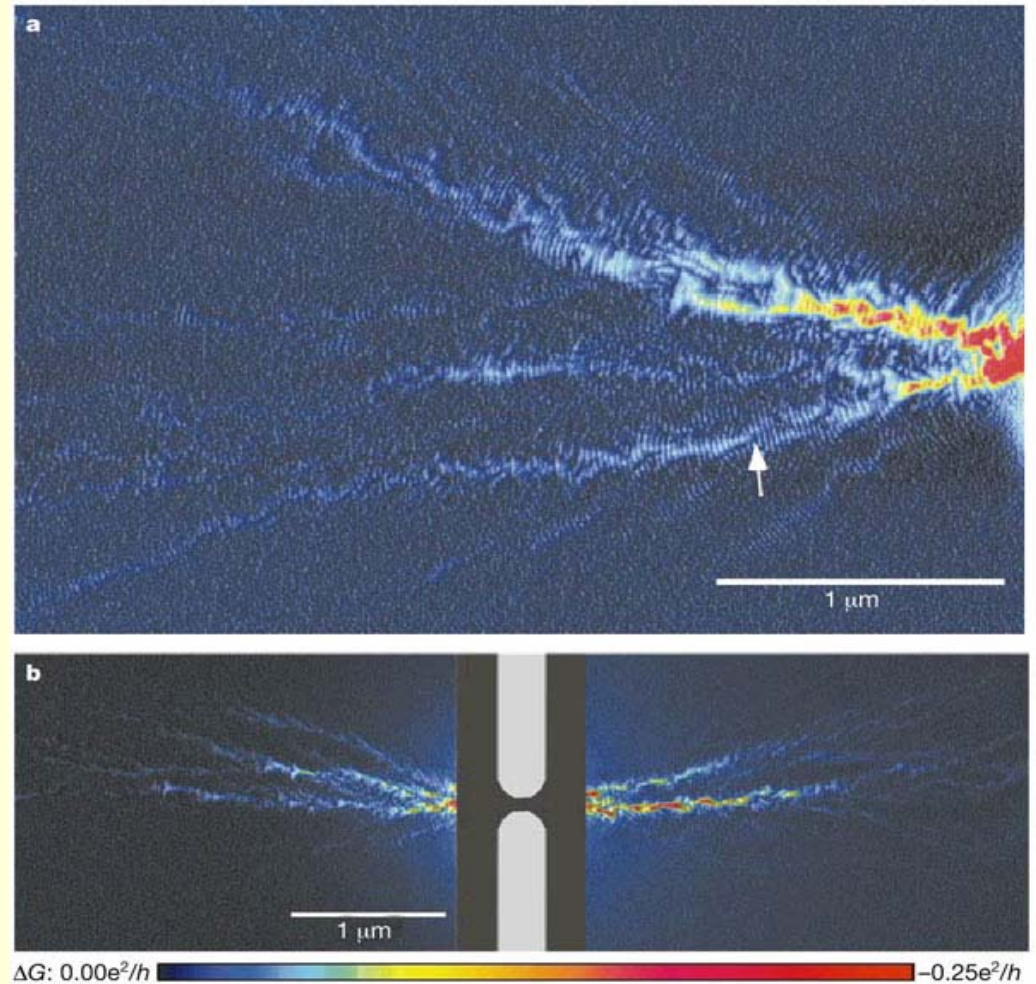
Conductance without the tip
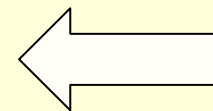
SGM images
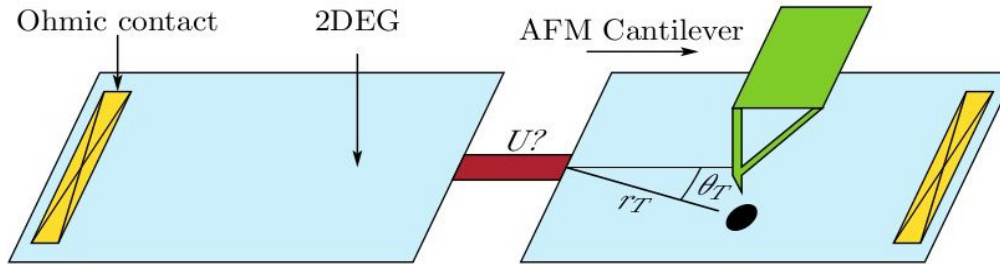## Conductance of the QPC as a function of the tip position

$\Delta g = g(\text{with tip}) - g(\text{without tip})$
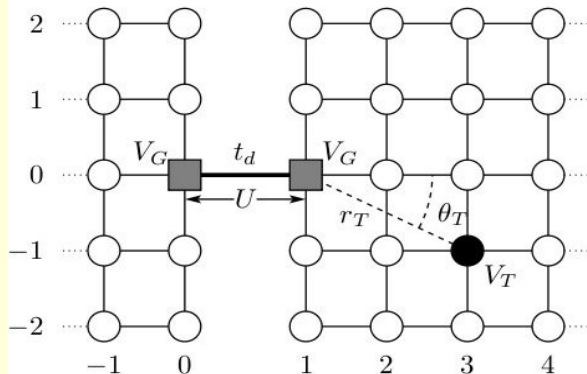
g(without tip)=2e²/h

Δg falls off with distance r from the QPC, exhibiting fringes spaced by λ_F/2

A lattice 2d model for SGM

$$H^{\text{nano}} = V_G(n_{0,0} + n_{1,0}) - t_d(c^{\dagger}_{0,0}c_{1,0} + \text{h.c.}) + Un_{0,0}n_{1,0}$$

- Nanosystem

  - Gate potential V_G
  - Hopping element t_d
  - Interaction U between two sites

- Tip potential V_T at (r_T, θ_T)

- Fermi-energy E_F (small E_F: no lattice effects)

- semi-infinite perfect leads

(Relative) Effect of the tip upon the conductance SGM images

relative changement of the conductance g with and without interaction

$$\frac{\Delta g}{g_0}(U = 0) \qquad \frac{\Delta g}{g_0}(U = 1.7)$$
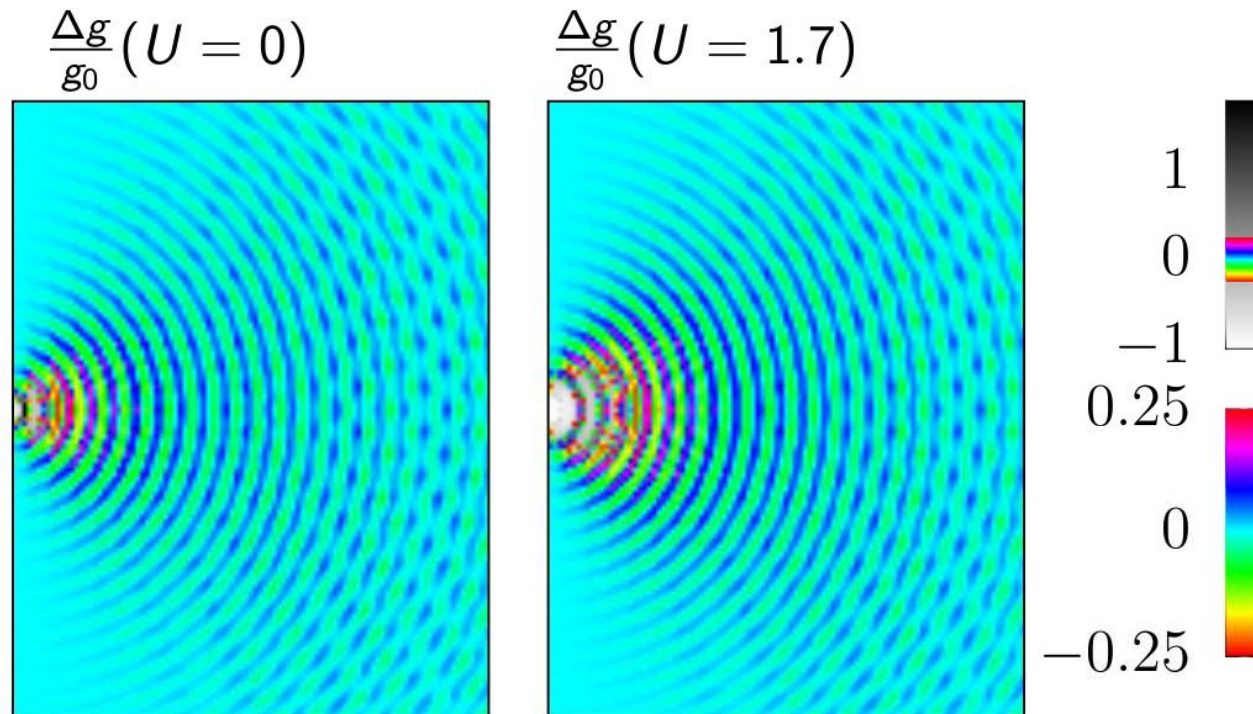
g_0: conductance without the tip

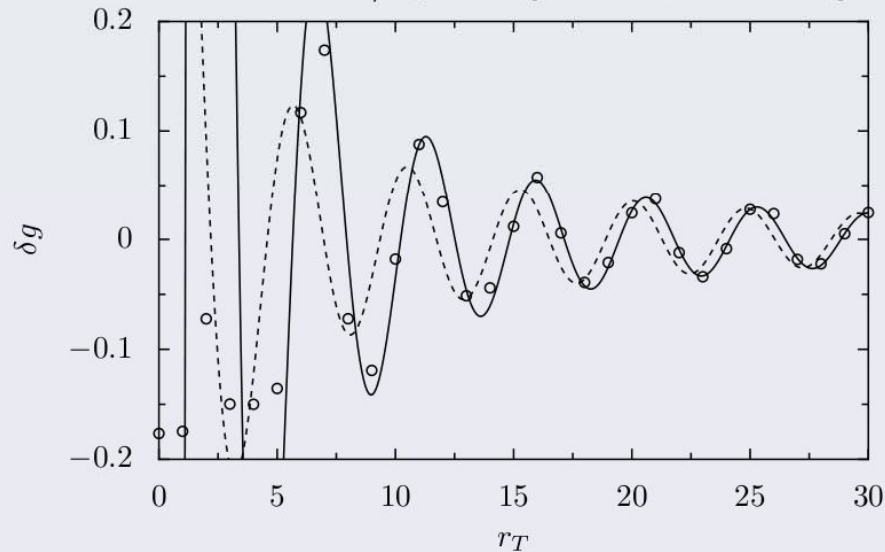$\Delta g = g(\text{with tip}) - g_0(\text{without tip})$

$\mathcal{L}_y = 301, \ E_F = -3.57, \ V_T = 2, \ t_d = 0.01, \ V_G = V_G^{\text{max}}$

With interaction, there is an additional $1/r_T^2$ decay (U=1.7)

Fit function

$$\delta g(r_t) = a_1 \frac{\cos(2k_F r_T + \delta_1)}{r_T} + a_2 \frac{\cos(2k_F r_T + \delta_2)}{r_T^2}$$

Dashed line: asymptotic $1/r_T$ decay
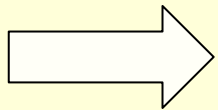Solid line: additional $1/r_T^2$ decay near the nanosystem

$a_1 = -0.67, \ a_2 = -7.60, \ \delta_1 = 1.66, \ \delta_2 = 0.12$

$\mathcal{L}_y = 301, \ E_F = -3.57, \ V_T = 2, \ t_d = 0.01, \ V_G = V_G^{\max}, \ \theta_T = 0$

Prédiction

L'effet de la pointe chargée du microscope AFM décroit plus lentement quand on éloigne du contact quantique la pointe chargée, si on mesure le thermovoltage au lieu de la conductance.

→ Intérêt d'une microscopie basée sur la mesure du thermovoltage